Available online at www.sciencedirect.com
ScienceDirect
Journal of Power Sources 177 (2008) 485–492
JOURNAL OF POWER SOURCES
www.elsevier.com/locate/jpowsour

Simple and fast fabrication of polymer template-Ru composite as a catalyst for hydrogen generation from alkaline $NaBH_4$ solution

Chan-Li Hsueh [a], Chuh-Yung Chen [b], Jie-Ren Ku [a], Shing-Fen Tsai [a], Ya-Yi Hsu [a], Fanghei Tsau [a], Ming-Shan Jeng [a,*]

[a] *Energy and Environment Research Laboratories (EEL), Industrial Technology Research Institute (ITRI), Building 64, 195 Sector 4, Chung Hsing Road, Chutung, Hsinchu 310, Taiwan*
[b] *Department of Chemical Engineering, National Cheng Kung University, Tainan City 701, Taiwan*

Received 8 October 2007; received in revised form 16 November 2007; accepted 19 November 2007
Available online 5 December 2007

Abstract

Polymer template-Ru composite (Ru/IR-120) catalyst was prepared using a simple and fast method for generating hydrogen from an aqueous alkaline $NaBH_4$ solution. The hydrogen generation rate was determined as a function of solution temperature, $NaBH_4$ concentration, and NaOH (a base-stabilizer) concentration. The maximum hydrogen generation rate reached 132 ml min^{-1} g^{-1} catalyst at 298 K, using a Ru/IR-120 catalyst that contained only 1 wt.% Ru. The catalyst exhibits a quick response and good durability during the hydrolysis of alkaline $NaBH_4$ solution. The activation energy for the hydrogen generation reaction was determined to be 49.72 kJ mol^{-1}.

Keywords: Hydrogen generation; Polymer template-Ru composite; Catalyst; $NaBH_4$

1. Introduction

Expanding global populations and increasing energy consumption are causing elevated carbon dioxide concentrations in the atmosphere, leading to global warming and climate change. Energy-generating devices, which do not contribute to such difficulties, are urgently required. As an energy-conversion device, a fuel cell directly converts the chemical energy of a supplied gas into electric energy at high efficiency and may help mitigate our energy and environmental problems in the future. Of various fuel cells, the proton exchange membrane fuel cell (PEMFC), which has a low operating temperature, high power density, high efficiency, rapid startup, fast response and zero emission, is considered the best candidate for vehicle and small-scale stationary applications. Since pure hydrogen serves as a fuel for PEMFC, a safe and economic method for hydrogen delivery and storage has become one of the most important issues in the success of large-scale PEMFC deployment.

The feasibility of storing and delivering hydrogen by chemical hydride (e.g., $NaBH_4$, KBH_4, LiH and NaH) has received considerable attention recently [1,2]. The chemical hydride is easy to transport and its hydrolysis controllably generates pure hydrogen. Among these hydrides, $NaBH_4$ is very attractive due to its various advantages, including relatively high hydrogen content (10.7 wt.%), stable and nonflammable alkaline solution, controllable hydrolysis reaction, environmentally friendliness, and renewability [3]. The hydrolysis of $NaBH_4$ generates hydrogen gas and water-soluble sodium metaborate, $NaBO_2$, in the presence of a suitable catalyst according to the following reaction [4].

$$NaBH_4 + 2H_2O \xrightarrow{\text{catalyst}} 4H_2 + NaBO_2 + \text{Heat} \quad (1)$$

This hydrolysis reaction proceeds at various rates that depend on the catalyst and its method of preparation. This work investigates heterogeneous ruthenium (Ru)-based catalyst that was supported on polymer templates [5,6]. The use of Ru as a catalyst for $NaBH_4$ hydrogen generation originated from the work of Brown and Brown [7], who examined a series of metal salts and found that Ru liberated H_2 most rapidly from borohydride solutions. Moreover, Ru catalysts are not consumed

* Corresponding author. Tel.: +886 3 5914223; fax: +886 3 5820230.
E-mail address: msjeng@itri.org.tw (M.-S. Jeng).

0378-7753/$ – see front matter © 2007 Elsevier B.V. All rights reserved.
doi:10.1016/j.jpowsour.2007.11.096

during hydrolysis and are reusable [5]. However, the limited surface area of the heterogeneous catalysts leads to lower catalytic activity. The use of metal nanoparticles with large surface area thus provides a potential route to increase the catalytic activity [8]. The hydrogen generation from the catalytic hydrolysis of sodium borohydride using water-dispersible ruthenium(0) nanoclusters as catalyst has been studied in literature [8,9]. Although ruthenium(0) nanoclusters catalyst can accelerate the catalytic activity, nano-sized metal particles would be very difficult to recover and handle at industrial level. Our previous studies have developed a simple and fast method for preparing CdS nanoparticles on a polymer template surface [10–12]. The polymer template is used to chelate Cd^{2+}, which form CdS nanoparticles after S^{2-} is added. The advantage of this technique is that all free Cd^{2+} in the solution can be removed by washing to prevent CdS nanoparticle from aggregation. The recovery and the handling of CdS nanoparticles also become easier with the polymer template. The above method is suitable not only for preparing CdS nanoparticles but also for other nanoparticles that can be prepared by reducing an appropriate metal ion polymer complex. This work applies this method to prepare polymer template-Ru composite as a catalyst for the generation of hydrogen from alkaline $NaBH_4$ solution. Additionally, the structures and catalytic activities of the Ru/IR-120 catalyst are characterized and discussed.

2. Experimental

2.1. Preparation of catalyst

Analytical reagent grade ruthenium(III) chloride hydrate (Sigma–Aldrich) and $NaBH_4$ (Riedel-de Haën) were used without further purification. The polymer templates, synthetic Amberlite IR-120 in hydrogen form (16–45 mesh size), were purchased from Supelco Chemical Co. (Bellefonte, PA, USA). Table 1 gives the properties of Amberlite IR-120. The volume capacity of Amberlite IR-120 was 1.89 eq l^{-1} based on analytical data provided by the manufacturer. Synthesis procedure of Ru/IR-120 catalyst is summarized below. Suitable amounts of ruthenium(III) chloride hydrate were dissolved in deionized water. A weighed amount of Amberlite IR-120 cationic exchange resin beads was added to the $RuCl_3$ solution that has been stirred for 1 h at the ambient temperature. After chelating with Ru^{3+}, Amberlite IR-120 surface structure transformed from $R_ZSO_3^-$–H^+ (R_Z = polymer matrix of the resin) into $(R_ZSO_3^-)_3$–Ru^{3+} (Ru^{3+}/IR-120). The resins were carefully washed repeatedly using deionized water to remove the soluble ions and then mixed with $NaBH_4$ solution as a reducing agent. Then, the resins were filtrated and washed repeatedly with deionized water and vacuum-dried at 90 °C to eliminate residual water and hydrogen. Finally, a polymer template-Ru composite (Ru/IR-120) catalyst was obtained.

Table 1
Properties of Amberlite IR-120

Type	Gel strong acid cation exchange resin
Active group	$–SO_3H$
Matrix	Styrene divinylbenzene copolymer
Ionic form as shipped	H^+
Standard mesh size (wet)	16–50 mesh
Mean particle size (mm)	0.5
Moist holding capacity	51.5%
Total exchange capacity meq ml^{-1} wet resin	1.89
mmol ml^{-1}	4.50

The surface morphology of the catalyst was observed using a scanning electron microscope (SEM; JEOL, JSM-6700F). The atomic composition of the catalyst surface was elucidated from energy dispersive spectra (EDS) using an Oxford INCA-400 spectrometer. X-ray diffraction (XRD) was performed using a powder diffractometer (Rigaku RX III) with Cu Kα radiation. The accelerating voltage and current were 40 kV and 20 mA, respectively. The Ru loadings in the catalysts were analyzed by thermogravimetric analysis (TGA; Dupont TA, Q50). Different atmospheres were used; (1) purge gas (in weight system)—argon with a flow rate of 100 cm^3 min^{-1} and (2) working gas—air with a flow rate of 90 cm^3 min^{-1}. The mass of the analyzed samples was around 300 mg. The following temperature program was applied; (1) an isothermic process at 30 °C for 60 s, (2) dynamic heating from 30 to 800 °C at a heating rate of 5 °C min^{-1}, (3) dynamic cooling from 800 to 30 °C, at a cooling rate of 20 °C min^{-1}. The specific surface area was estimated using an BET (Brunauer Emmett and Teller) analyzer (ASAP 2010, Micromeritics Inst. Co.). Initially, the aerogels were degassed at 300 °C and the N_2 adsorption–desorption isotherms were obtained at 77 K. The specific surface area was then calculated using BET method.

2.2. Generation of hydrogen

The catalytic activity of Ru/IR-120 catalyst was determined by measuring the amount of hydrogen that was generated by the hydrolysis of sodium borohydride. Fig. 1 shows the experimental setup. The temperature of the water bath was maintained constant with a stability of ±0.1 °C using a thermostatic circulator. Total solution volume in all experiments was 15 ml. The $NaBH_4$ solution was thermostatically maintained at a preset temperature in the sealed flask, in which the solution was stirred vigorously. The starting point of the reaction was defined as the time when a certain quantity of Ru/IR-120 catalyst was added to the flask. A graduated glass column filled with water was connected to the

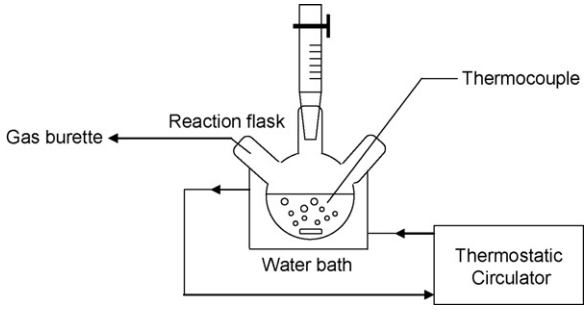

Fig. 1. Schematic of the experimental setup.

top outlet of the flask as a gas burette. The volume of hydrogen gas evolved was measured from the water level change in the column.

3. Results and discussion

3.1. Characterization of Ru/IR-120 catalyst

This investigation aims to develop a simple and fast method for preparing the polymer template-Ru composite as a catalyst for hydrogen generation from alkaline $NaBH_4$ solution. Fig. 2 displays photographs of the fabrication of the catalyst. Fig. 2a shows the original Amberlite IR-120 cationic exchange resin beads. The surface color of the original resin beads is yellowish-brown. After the original resin beads had been chelated with

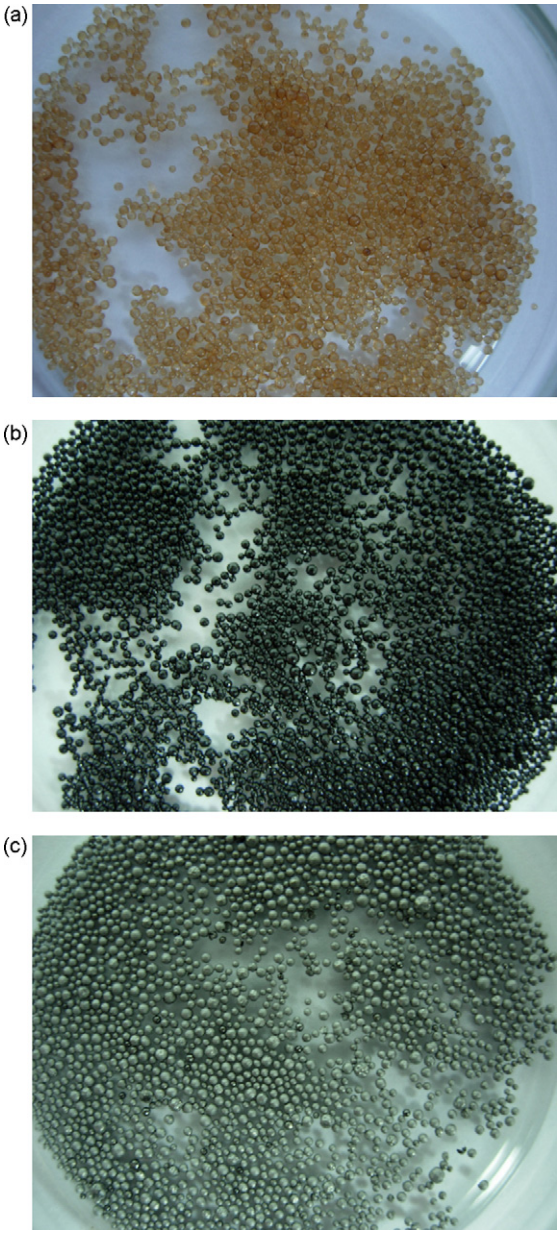

Fig. 2. Photographs of (a) IR-120; (b) Ru^{3+}/IR-120; (c)Ru/IR-120.

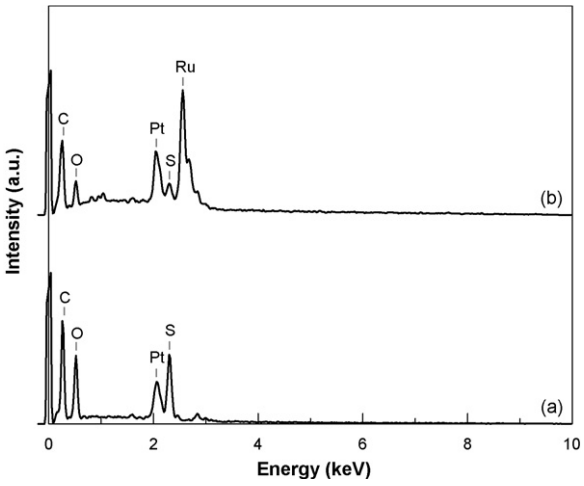

Fig. 3. EDS spectra of (a) IR-120 and (b) Ru/IR-120.

Ru^{3+}, the surface color turned from yellowish-brown to black (Ru^{3+}/IR-120), as presented in Fig. 2b. The surface color of Ru^{3+}/IR-120 became silvery white (Fig. 2c) immediately upon contact between the reducing agent and Ru^{3+}/IR-120.

Fig. 3 presents the EDS of the original IR-120 resin beads (curve a) and that of the Ru/IR-120 catalyst (curves b). Curve a reveals that C, O and S are the dominant elements detected on the surface of IR-120. However, curve b indicates that only Ru was added to the surface of IR-120 after reduction. Table 2 presents the quantitative surface chemical compositions of the Ru/IR-120 catalyst, determined by EDS. Fig. 4 depicts the low-magnified EDS mapping and SEM images of the Ru/IR-120 catalyst. The area enclosed by the dotted lines in the SEM image corresponds to the area of the EDS mapping images. The result clearly reveals that Ru is uniformly distributed on Ru/IR-120 surface.

Fig. 5 presents SEM micrographs of IR-120, Ru^{3+}/IR-120 and Ru/IR-120. The low-magnified (50×) SEM images demonstrate that the particle sizes of Ru^{3+}/IR-120 (Fig. 5c) and Ru/IR-120 (Fig. 5e) were very close to those of IR-120 (Fig. 5a), implying that the active layer (Ru) represented a small proportion of all particles. Fig. 5b and d indicates that the IR-120 and Ru^{3+}/IR-120 surfaces are smooth under the highly magnified SEM images (50,000×). However, after reduction reaction, Ru nanoparticles aggregate on the Ru/IR-120 surface (Fig. 5f). The BET surface area of the Amberlite IR-120 resin is only 2.52 $m^2\,g^{-1}$ because Amberlite IR-120 resin is gel-type and nonporous. After reduction reaction produces Ru/IR-120, the BET surface area moderately increases to 18.07 $m^2\,g^{-1}$. The

Table 2
Surface weight and atomic percentage of the elements present in polymer template (Amberlite IR-120 resin) and catalyst (Ru/IR-120) by EDS

Elements	Amberlite IR-120 resin		Ru/IR-120	
	wt.%	at.%	wt.%	at.%
C	53.17	65.30	10.35	32.73
O	28.49	26.26	15.05	35.71
S	18.34	8.44	4.38	5.18
Ru	0	0	70.22	26.38

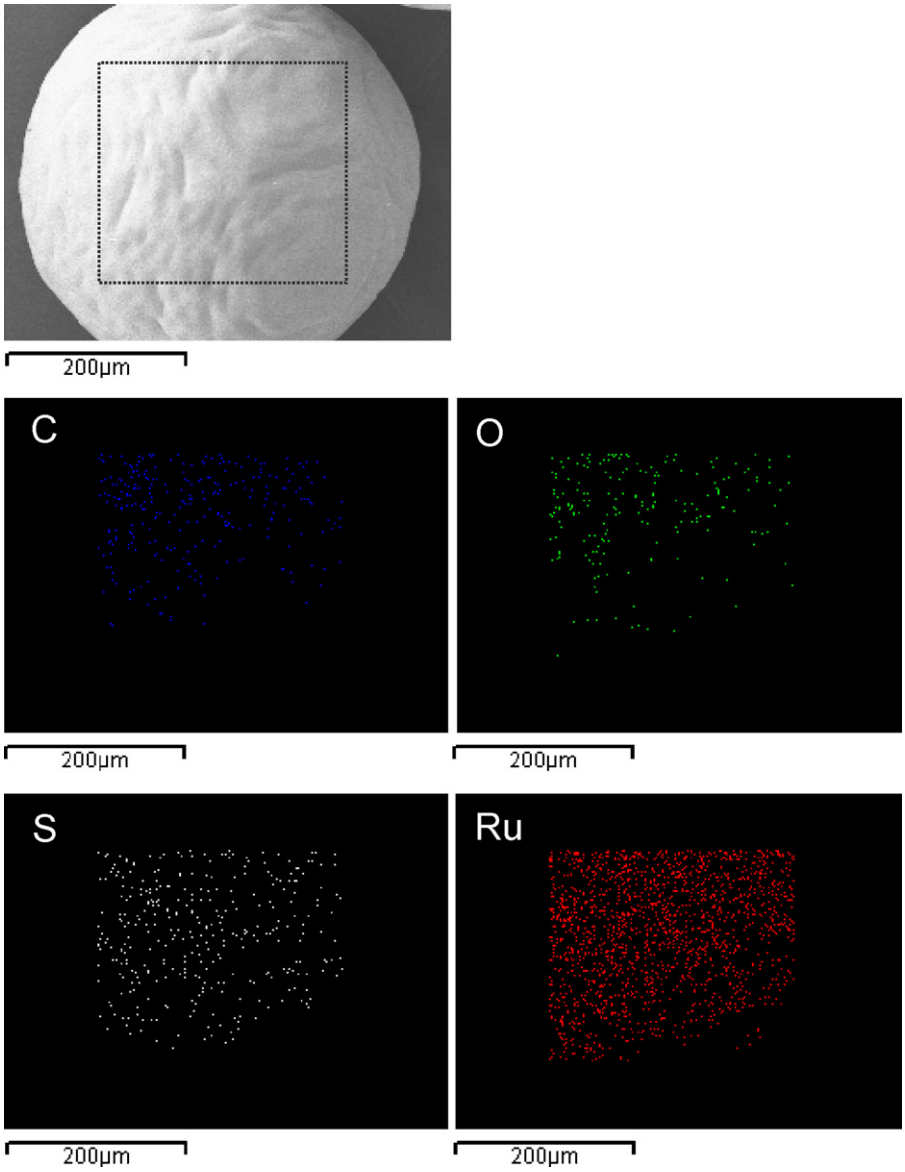

Fig. 4. SEM and EDS mapping of Ru/IR-120 catalyst and the elemental distributions of C, O, S and Ru. Scale bar is 200 μm.

surface area of Ru/IR-120 does not increase substantially due to Ru nanoparticles aggregation on the Ru/IR-120 surface. An effective method to disperse Ru nanoparticles on IR-120 surface is under development, and will be published later along with the structure and characteristics of the Ru/IR-120 catalyst under various reduction conditions.

Fig. 6a–c displays the XRD patterns of IR-120, Ru^{3+}/IR-120 and Ru/IR-120, respectively. The pure Ru pattern was taken from the Joint Committee on Powder Diffraction Standards (JCPDS) diffraction files. The main diffraction peaks appear at $2\theta = 38.4°$, 42.2°, 44°, 58.3°, 69.4° and 78.4°. The peak at $2\theta = 44°$ is most intense. Fig. 6a and b demonstrates that IR-120 and Ru^{3+}/IR-120 have amorphous structure. However, Ru/IR-120 yields a weak diffraction peak at $2\theta = 44°$, revealing that the Ru loadings in Ru/IR-120 may be small. Therefore, TGA measurements were made to quantify the amount of Ru in the Ru/IR-120 catalyst. Fig. 7 plots the TGA curves of both IR-120 and Ru/IR-120. A careful investigation of the curves yields the following observations.

(i) The profile of Ru/IR-120 differs greatly from that of IR-120, because of the Ru presence in Ru/IR-120.
(ii) Curve a in Fig. 7 shows TGA oxidative pyrolysis results of IR-120 resin. The resin decomposition from 30 to 800 °C proceeds in three stages—first by water evaporation, second by active group decomposition, and finally by polymer matrix combustion. These findings agree with the previous results obtained under oxidizing conditions [13].
(iii) Curve b in Fig. 7 shows TGA results of Ru/IR-120 catalyst under oxidative pyrolysis. Loading IR-120 resin with Ru increases its degradation temperature. The delay in degradation may be attributed to the stable nature of inorganic Ru, which stabilizes the resin during heating.

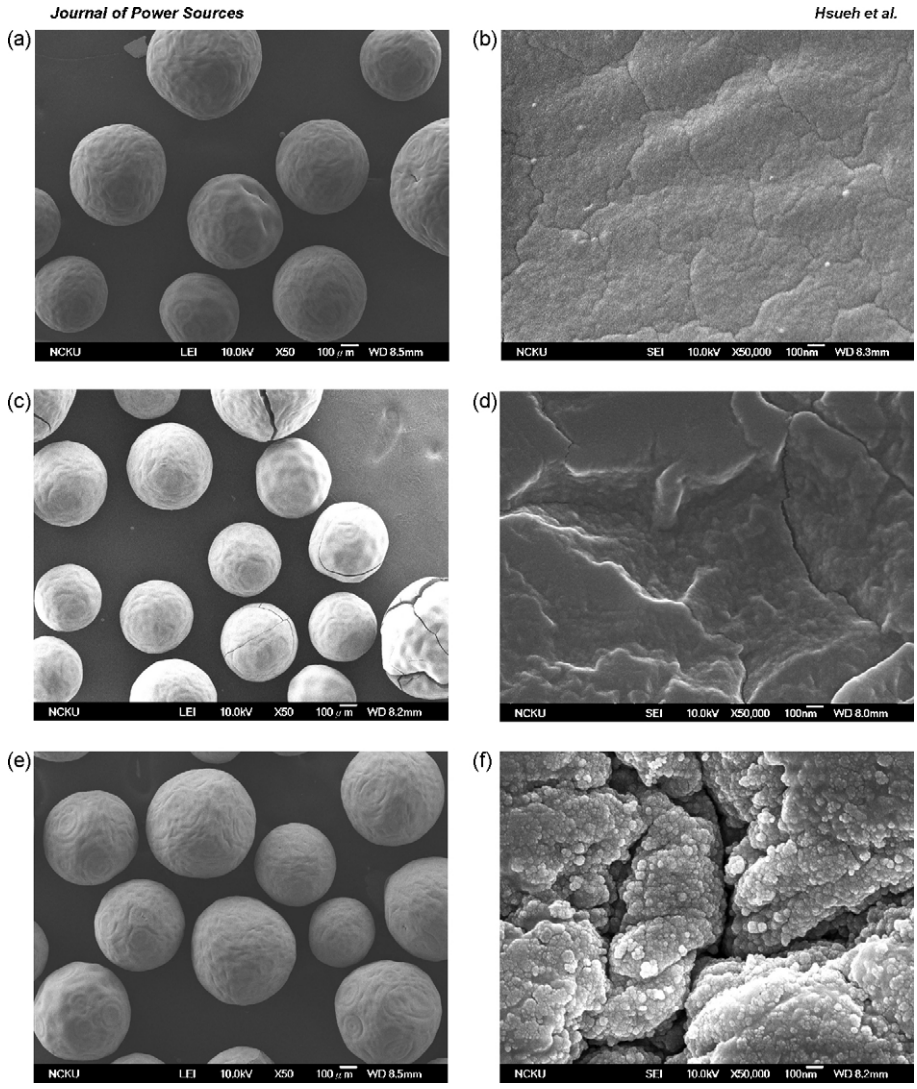

Fig. 5. Scanning electron micrographs of (1) IR-120: (a) 50×; (b) 50,000×, (2) Ru^{3+}/IR-120: (c) 50×; (d) 50,000× and (3) Ru/IR-120: (e) 50×; (f) 50,000×.

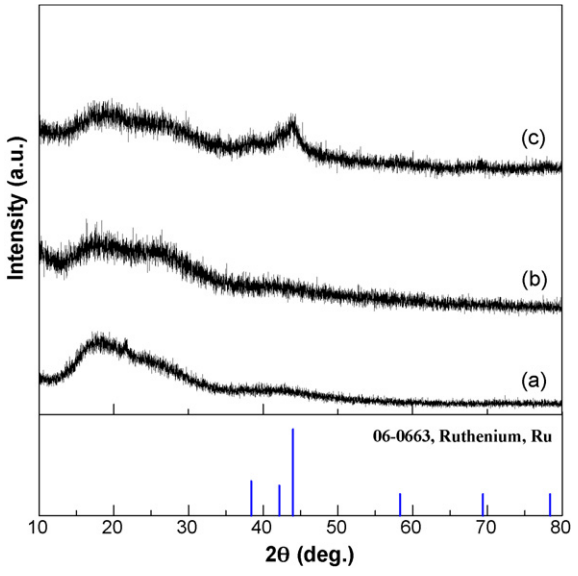

Fig. 6. X-ray powder diffraction patterns (a) IR-120; (b) Ru^{3+}/IR-120; (c) Ru/IR-120.

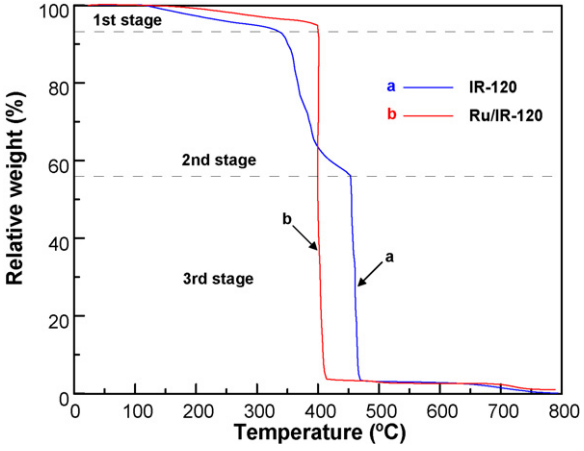

Fig. 7. TGA curves of (a) IR-120 and (b) Ru/IR-120.

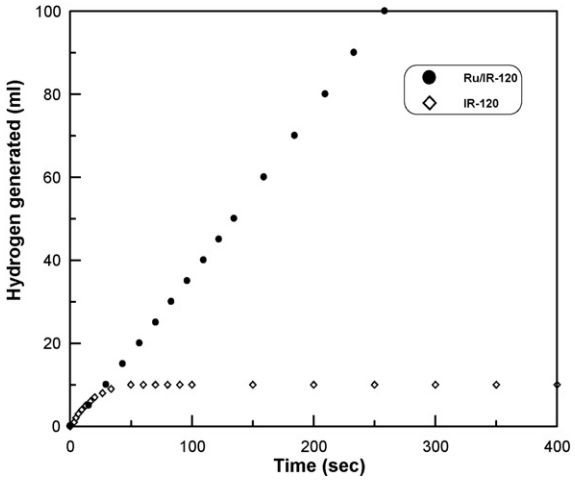

Fig. 8. Hydrogen generation rate measured from 5 wt.% $NaBH_4$ + 1 wt.% NaOH solution at 25 °C using 200 mg of Ru/IR-120 catalyst and 200 mg of IR-120 resin.

(iv) According to the TGA curves, the Ru/IR-120 catalyst yields a 1% final residue, while the original IR-120 resin yields 0%. The residual percentage of the Ru/IR-120 confirms the presence of Ru.

3.2. Catalytic activities

The Ru/IR-120 catalyst was evaluated in terms of milliliters of H_2 generated per second-gram catalyst, as follows.

3.2.1. Comparison of catalysis efficacy between IR-120 resin and Ru/IR-120

The Amberlite IR-120 resin is a strong acidic cation exchange resin. Sodium borohydride hydrolysis can be accelerated not only by catalysts but also by acid [8]. In order to understand the catalysis of IR-120 resin for the generation of H_2 from alkaline $NaBH_4$ solution, a comparison of catalysis efficacy between IR-120 resin and Ru/IR-120 was conducted. The reactions were carried out under the following conditions: 5 wt.% $NaBH_4$ + 1 wt.% NaOH solution at 25 °C. As Fig. 8 reveals, the effect of IR-120 resin on hydrogen generation was considerably smaller than that of Ru/IR-120. The catalysis effect of IR-120 resin for hydrogen generation from alkaline $NaBH_4$ solution is therefore neglected in this study.

3.2.2. Effect of NaOH concentration on H_2 generation

The effect of NaOH concentration on the H_2 generation rate was studied using 10 wt.% $NaBH_4$ + x wt.% NaOH solutions, where x = 1, 5, 10, and 15, at 298 K using 200 mg of Ru/IR-120 catalyst, by measuring the cumulative volumes of hydrogen. Fig. 9 plots the results. As the NaOH concentration increases from 1 to 15%, the initial H_2 generation rate decreases from 120 to a minimum of 31 ml min^{-1} g^{-1} catalyst. These findings are consistent with the previous results of Amendola et al. [6]. However, the results differ from those of Hua et al. [14] and Jeong et al. [15], who reported that the use of an $NaBH_4$ solution with high NaOH concentration generates hydrogen at a higher rate than using an Ni or Co-B catalyst. These results indicate that

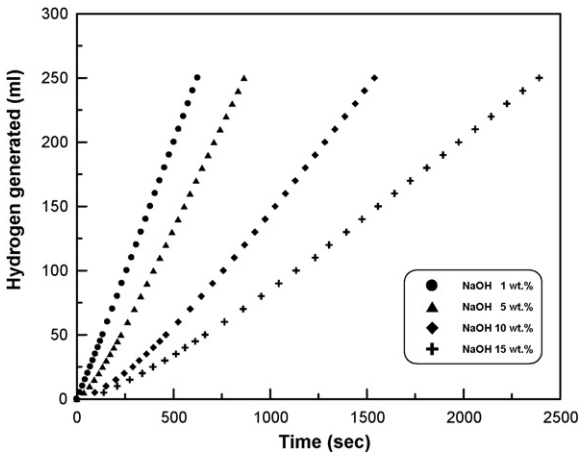

Fig. 9. Volume of hydrogen generated as a function of time in different NaOH concentrations (25 °C, 10 wt.% $NaBH_4$ solution, 200 mg Ru/IR-120 catalyst).

the effect of NaOH concentration on $NaBH_4$ hydrolysis depends greatly on the catalysts. The effect associated with the Ru/IR-120 catalyst differs markedly from that associated with Ni and Co-B catalysts.

3.2.3. Effect of $NaBH_4$ concentration on H_2 generation rates

The effect of $NaBH_4$ concentrations on the H_2 generation rate from x wt.% $NaBH_4$ + 1 wt.% NaOH solutions, where x = 1, 5, 10, 15, 25, was examined at 298 K using 200 mg of Ru/IR-120 catalyst by measuring the cumulative volumes of hydrogen. Fig. 10 plots the results. As the weight percentage of $NaBH_4$ increases, the initial H_2 generation rate increases, reaching a maximum in the range of 1–5% $NaBH_4$. Note that the weight percentage of $NaBH_4$ that produces this maximum also depends on the weight percentage of NaOH. As the $NaBH_4$ concentration in the solution increased from 5 to 25 wt.%, the initial H_2 rates decreased from 132 to 32 ml min^{-1} g^{-1}. Amendola et al. [6] reported that, for a Ru catalyst, the hydrogen from $NaBH_4$ + NaOH solution decreased as the $NaBH_4$ concentra-

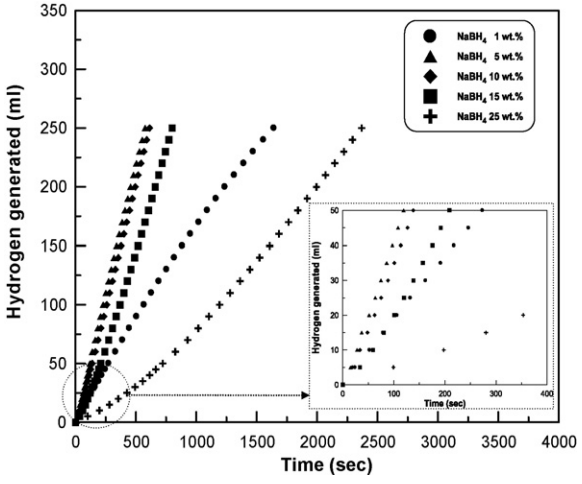

Fig. 10. Volume of hydrogen generated as a function of time in different $NaBH_4$ concentrations (25 °C, 1 wt.% NaOH solution, 200 mg Ru/IR-120 catalyst).

Table 3
Comparisons of H_2 generation performance between various catalysts

Catalyst	Initial temperature for H_2 generation (°C)	$NaBH_4$ concentration (wt.%)	Average H_2 generation rate (ml min^{-1} g^{-1})	Reference
5 wt.% Ru on IRA-400	32.5	7.5	601	[6]
5 wt.% Ru on IRA-400	40	7.5	1098	[6]
9 wt.% Co on γ-Al_2O_3	30	5	220[a]	[3]
1 wt.% Ru on IR-120	5	5	23	This paper
1 wt.% Ru on IR-120	15	5	48	This paper
1 wt.% Ru on IR-120	25	5	132	This paper
1 wt.% Ru on IR-120	35	5	194	This paper
1 wt.% Ru on IR-120	45	5	392	This paper
1 wt.% Ru on IR-120	55	5	585	This paper

[a] Maximum H_2 generation rate.

tion increased. They attributed these results to increased solution viscosity.

3.2.4. Effect of solution temperature on H_2 generation rates

Fig. 11 plots H_2 generation rates of 5 wt.% $NaBH_4$ + 1 wt.% NaOH (and 94 wt.% water solutions) at various temperatures in the 5–55 °C range. As expected, the H_2 generation rate increases as the temperature increases. The comparisons of H_2 generation performances of Ru/IR-120 catalyst with those of other catalysts are listed in Table 3. The H_2 generations rate of Ru/IR-120 catalyst is smaller than IRA-400-supported Ru or γ-Al_2O_3-supported Co. However, the Ru loading in the catalysts used in this paper is only 1 wt.%.

Additionally, Fig. 11 demonstrates that the hydrogen volumes increase almost linearly with reaction time, suggesting that the reaction rate is constant during a hydrolysis reaction such that the reaction can be regarded as zero-order. The reaction rate equation of the zero-order Ru/IR-120 catalyst reaction can be written as [3],

$$r = k_0 \exp\left(\frac{-E}{RT}\right) \quad (2)$$

where r is the reaction rate (mol min^{-1} g^{-1}), k_0 is the reaction constant (mol min^{-1} g^{-1}), E is the activation energy of the reaction, R is the gas constant, and T is the reaction temperature. The slope of ln r versus $1/T$ therefore equals to E/R. Fig. 12 plots the curve of ln r against $1/T$ for the Ru/IR-120 hydrogen generation reaction. The activation energy is 49.72 kJ mol^{-1}, as calculated from the slope of the fitted straight line in Fig. 12. This activation energy is lower than the value, 56 kJ mol^{-1}, reported by Amendola et al. [6], who used an IRA 400-supported Ru catalyst in more concentrated $NaBH_4$ (7.5 wt.%) with the same NaOH concentration (1 wt.%). The activation energies of $NaBH_4$ hydrolysis reaction augmented by other metal catalysts, as presented by Kaufman and Sen (Co, 75 kJ mol^{-1}; Ni, 71 kJ mol^{-1}; Raney Ni, 63 kJ mol^{-1}) [16], are also higher than the activation energy reported in this study.

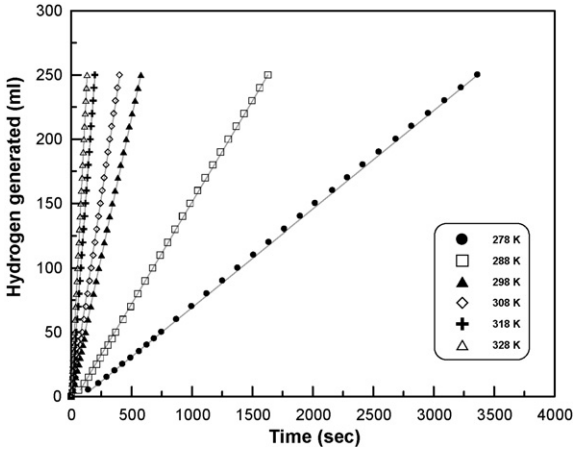

Fig. 11. Volume of hydrogen generated as a function of time in different solution temperatures (5 wt.% $NaBH_4$ + 1 wt.% NaOH solution, 200 mg Ru/IR-120 catalyst).

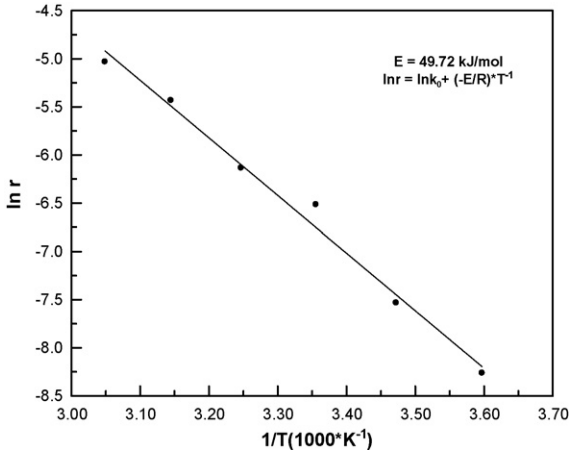

Fig. 12. ln r vs. $1/T$ plot obtained from the data shown in Fig. 11 for the hydrogen generation reaction using a Ru/IR-120 catalyst.

4. Conclusion

A simple and fast method for fabricating a polymer template-Ru composite as a catalyst, Ru/IR-120, was developed for hydrolyzing sodium borohydride from its alkaline solution. This method is suitable for the preparation of not only polymer template-Ru composite but also other polymer template-metal composites, such as Co, Ni, Fe and Cu. A Ru loading as low as 1 wt.% in the Ru/IR-120 was achieved using this technique. When a Ru/IR-120 catalyst that contains 1 wt.% Ru was used, a maximum hydrogen generation rate of 132 ml min^{-1} g^{-1} from

5 wt.% $NaBH_4$ + 1 wt.% NaOH solution at 25 °C was obtained. There is still room for improvement for the dispersion of Ru nanoparticles on IR-120 surface, which would markedly improve the hydrogen generation rate further. Moreover, as the solution temperature increases, the hydrogen generation rate increases. The activation energy of the $NaBH_4$ hydrolysis reaction using the Ru/IR-120 catalyst was determined to be 49.72 kJ mol^{-1}, lower than the activation energies of other catalysts reported in the literature.

Acknowledgements

The authors would like to thank the Bureau of Energy, Ministry of Economic Affairs of Republic of China, for financially supporting this research under Contract No. 6455DC5220.

References

[1] C. Wu, F. Wu, Y. Bai, B. Yi, H. Zhang, Mater. Lett. 59 (2005) 1748–1751.
[2] N. Sifer, K. Gardner, J. Power Sources 132 (2004) 135–138.
[3] W. Ye, H. Zhang, D. Xu, L. Ma, B. Yi, J. Power Sources 164 (2007) 544–548.
[4] H.I. Schlesinger, H.C. Brown, A.B. Finholt, J.R. Gilbreath, H.R. Hockstra, E.K. Hydo, J. Am. Chem. Soc. 75 (1953) 215.
[5] S.C. Amendola, S.L. Sharp-Goldman, M.S. Janjua, M.T. Kelly, P.J. Petillo, M. Binder, J. Power Sources 85 (2000) 186–189.
[6] S.C. Amendola, S.L. Sharp-Goldman, M.S. Janjua, N.C. Spencer, M.T. Kelly, P.J. Petillo, M. Binder, Int. J. Hydrogen Energy 25 (2000) 969–975.
[7] H.C. Brown, C.A. Brown, J. Am. Chem. Soc. 84 (1962) 1493.
[8] S. Özkar, M. Zahmakıran, J. Alloys Compd. 404–406 (2005) 728–731.
[9] M. Zahmakıran, S. Özkar, J. Mol. Catal. A: Chem. 258 (2006) 95–103.
[10] Y.C. Chu, C.C. Wang, C.Y. Chen, J. Membr. Sci. 247 (2005) 201–209.
[11] Y.C. Chu, C.C. Wang, C.Y. Chen, Nanotechnology 16 (2005) 58–64.
[12] Y.C. Chu, C.C. Wang, C.Y. Chen, Nanotechnology 16 (2005) 376–385.
[13] R.S. Juang, T.S. Lee, J. Hazard. Mater. B92 (2002) 301–314.
[14] D. Hua, Y. Hanxi, A. Xingping, C. Chuansin, Int. J. Hydrogen Energy 28 (2003) 1095–1100.
[15] S.U. Jeong, R.K. Kim, E.A. Cho, H.-J. Kim, S.-W. Nam, I.-H. Oh, S.-A. Hong, S.H. Kim, J. Power Sources 144 (2005) 129–134.
[16] C.M. Kaufman, B. Sen, J. Chem. Soc., Dalton Trans. (1985) 307–313.